

Drag reduction characteristics of heated spheres falling into water

Jia-Chuan Li(李佳川), Ying-Jie Wei(魏英杰), Cong Wang(王聪), Wei-Xue Xia(夏维学)

Citation: Chin. Phys. B . 2018, 27(12): 124703. **doi:** 10.1088/1674-1056/27/12/124703
Journal homepage: http://cpb.iphy.ac.cn; http://iopscience.iop.org/cpb

What follows is a list of articles you may be interested in

Experimental investigation on underwater drag reduction using partial cavitation

Bao Wang(王宝), Jiadao Wang(汪家道), Darong Chen(陈大融), Na Sun(孙娜), Tao Wang(王涛)

Chin. Phys. B . 2017, 26(5): 054701. **doi:** 10.1088/1674-1056/26/5/054701

Predetermined control of turbulent boundary layer with a piezoelectric oscillator

Xiao-Bo Zheng(郑小波), Nan Jiang(姜楠), Hao Zhang(张浩)

Chin. Phys. B . 2016, 25(1): 014703. **doi:** 10.1088/1674-1056/25/1/014703

A new mixed subgrid-scale model for large eddy simulation of turbulent drag-reducing flows of viscoelastic fluids

Li Feng-Chen, Wang Lu, Cai Wei-Hua

Chin. Phys. B . 2015, 24(7): 074701. **doi:** 10.1088/1674-1056/24/7/074701

Influence of polymer additives on turbulent energy cascading in forced homogeneous isotropic turbulence studied by direct numerical simulations

Li Feng-Chen, Cai Wei-Hua, Zhang Hong-Na, Wang Yue

Chin. Phys. B . 2012, 21(11): 114701. **doi:** 10.1088/1674-1056/21/11/114701

Drag reduction characteristics of heated spheres falling into water*

Jia-Chuan Li(李佳川), Ying-Jie Wei(魏英杰)†, Cong Wang(王聪), and Wei-Xue Xia(夏维学)

School of Astronautics, Harbin Institute of Technology, Harbin 150001, *China*

(Received 13 July 2018; revised manuscript received 29 August 2018; published online 10 November 2018)

We experimentally investigate the drag reduction characteristics of heated spheres falling into water by using a high-speed camera. In 25-°C water, with the increase of the sphere temperature the average velocity increases to a maximum value at a temperature of 400 °C and then decreases until the temperature reaches 700 °C, the average velocity will increase while the sphere temperature continually rises until the temperature reaches 900 °C. The average and the maximum velocity of the heated sphere are larger than those of the room-temperature sphere. The flow separates at the rear of the heated sphere, leading to low pressure drag. The drag reduction effect of the stable film boiling is lower than that of the nucleate boiling. In the nucleate boiling regime, the average velocity decreases with the increase of water temperature, the drag of the sphere with gentle boiling intensity is smaller. The vapor layer formed in the stable film boiling regime can improve the stability of the fall trajectory. The intense turbulence caused by the nucleate boiling can make the sphere largely deviate from rectilinear motion.

Keywords: drag reduction, boiling, bubbles, vapor layer

PACS: 47.55.dp, 47.54.De, 47.85.lb **DOI:** 10.1088/1674-1056/27/12/124703

1. Introduction

Drag reduction is an important problem in hydrodynamics for its close correlation with the applications in the fields of military, navigation, chemical engineering, etc.

There are many methods to reduce drag, such as by using polymeric additives,[1–3] microbubble injection,[4,5] exploiting supercavitation or partial cavitation,[6,7] and hydrophobic coating.[8–10] These methods reduce drag mainly by changing the surface characteristics of the object or by changing the viscosity of the fluid near the object.

Heating the object to a temperature above the boiling point, the surrounding liquid will vaporize. If the surface temperature is not high enough, bubbles will be formed around the object, and this boiling process is called nucleate boiling. If the temperature of the surface is significantly higher than the liquid's boiling point, bubbles will immediately converge to form a vapor layer separating the object from the surrounding liquid, and this boiling process is called film boiling.

The vapor layer can be used to reduce the skin friction between an object surface and a fluid.[11–14] Saranadhi[13] heated a superhydrophobic surface of the inner rotor of a custom Taylor–Couette apparatus at a low superheat temperature to establish a stable and continuous vapor layer between the surface and the surrounding water. The vapor layer lubricates the interface, leading the friction drag to decrease. In their experiments, the skin friction can be reduced by 80% to 90% against unheated surface.

Recent studies have presented that the vapor layer formed in the film boiling regime can also be used to reduce the pressure drag caused by the difference between pressures in the front and the rear of the object.[15–20] Vakarelski *et al.*[17] investigated the drag reduction effects of the vapor layer when a free-falling sphere reached its terminal velocity in a fully fluorinated liquid with a low boiling point and a low latent heat of vaporization against water. They conducted the experiments in the subcritical range of Reynolds number, where the pressure-induced drag accounted for more than 95%. The hydrodynamic drag could be reduced by over 85% as shown by Vakarelski *et al.*[17] Therefore the vapor layer had to significantly change the pressure drag. For a sphere falling into a liquid, the farther the flow separation location away from the bottom of the sphere, the lower the pressure drag is. Vakarelski *et al.*[17,19,20] presented that the flow separation occurs at about the sphere's equator for an unheated sphere, the lubrication of the vapor layer in the film boiling regime can make the separation point move to the rear of the sphere, resulting in the reduction of pressure drag.

Nucleate boiling was also formed in the Vakarelski *et al.*'s study.[17–19] The height of the water tank was between 1.6 m and 2 m. They calculated the drag coefficient by using the terminal velocity of the sphere when it was close to the bottom of the tank. For stable film boiling, a vapor layer still exists around the sphere during the falling process. The heat transfer intensity in the nucleate boiling regime is at least one order higher that in the stable film boiling regime. The intensity of nucleate boiling greatly decreases when the sphere reaches the bottom of the water tank. In Vakarelski *et al.*'s experiments,[17–19] nucleate boiling had only a small effect on the terminal velocity of the sphere. The drag reduction of nucleate boiling may be underestimated by using the Vakarelski

*Project supported by the National Natural Science Foundation of China (Grant No. 11672094).

†Corresponding author. E-mail: weiyingjie@gmail.com

© 2018 Chinese Physical Society and IOP Publishing Ltd

et al.'s experimental method.[17–19]

In the present article, we show the average velocity of sphere in both nucleate boiling and film boiling regimes during the whole falling process into water with different temperatures. We investigate the sphere and water temperature effect on the drag reduction. Using a water tank with a height of 0.6 m, the duration of each experimental drop of the spheres is less than 0.7 s. The nucleate boiling can maintain a certain boiling intensity during the fall. For most trials, we find that the nucleate boiling has better drag reduction effect than the stable film boiling. We present the variation of falling velocity with time for a room-temperature sphere, a sphere in nucleate boiling regime and a sphere in stable film boiling regime and discuss the stabilities of the fall trajectory for the three cases.

2. Experimental setup

Our experimental setup is shown in Fig. 1. The spheres used were silicon nitride ceramic spheres. The density of the sphere was $\rho_s = 3200$ kg/m^3. The radius of the sphere was $R = 10$ mm within an error less than 13 nm. The change of temperature had little effect on the structure and size of the sphere. The working temperature of the sphere could reach 1200 °C or even higher. The water tank was made of tempered glass. The height of the tank was 61 cm, the cross-section size was 30 cm×30 cm. The water surface was kept at a height of 60 cm in the experiments. The spheres were washed by water and alcohol prior to the experiments.

The sphere was heated in a muffle furnace and kept for more than an hour after the temperature displayed on the temperature controller had reached the preset value. The water was heated by using a heating device and stirred to obtain uniform temperature. When the water temperature reached the preset value, the sphere was taken out of the muffle furnace and released slightly above the water surface. In our experiments, the water temperatures were in a range of 25 °C–95 °C and the sphere temperatures were in a range of 25 °C–900 °C.

A high-speed camera (Photron Fastcam SA-X) was used to capture the falling processes of the spheres. The falling velocities were determined by the video clips. Uniform back lighting was achieved by a group of 6 × 500-W light sources illuminating a diffuser screen. A foreground light-emitting diode (LED) light was used to observe the flow conditions on the sphere surface.

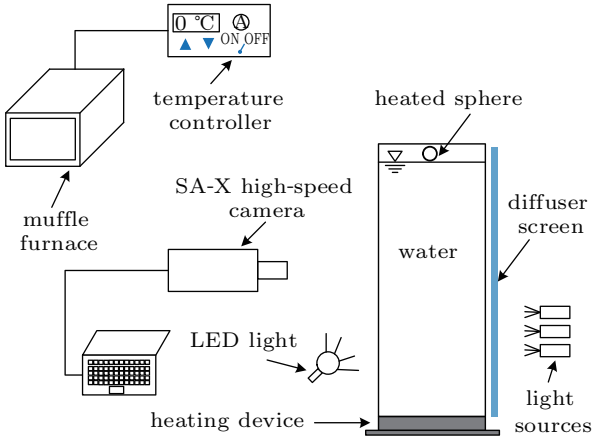


Fig. 1. (color online) Schematic diagram of the experimental setup used.

3. Results and discussion

We calculate the average velocity of a sphere from immerging into water to reaching the bottom of the water tank by using the video clips. Table 1 shows the average velocities of the whole falling processes for three cases with different water and sphere temperatures. We repeated 5 times for each case. The V_{ave} is the mean value of average velocities for each case and σ is the standard deviation. The value of σ for each case is small compared with the value of V_{ave}. So, our experimental results have better repeatability. We repeat at least three times for all trials, and we just present the mean value of the averaged velocities in the following subsections.

Table 1. Average velocities for three cases with different water and sphere temperatures.

No.	T_w/°C	T_s/°C	Average velocity/(m/s)						σ
			Exp. 1	Exp. 2	Exp. 3	Exp. 4	Exp. 5	V_{ave}	
1	25	25	0.933	0.941	0.936	0.932	0.938	0.936	0.003
2	25	400	1.206	1.209	1.189	1.196	1.195	1.199	0.007
3	95	500	1.03	1.038	1.041	1.041	1.03	1.036	0.005

3.1. Influence of the sphere temperature

In Fig. 2, we present the effect of sphere temperature on the average velocity of the sphere falling into water, in which case the water temperature is 25 °C. We find that the averaged velocities of the heated spheres are larger than those of the room-temperature spheres. Heating a sphere can reduce the drag of the sphere moving into water. The average velocity does not always increase with sphere temperature increasing. In our experiments, the average velocity increases until the temperature of the sphere reaches 400 °C and then decreases until the temperature of the sphere reaches 700 °C, the average velocity will increase while the sphere temperature

continues rising. The maximum averaged velocity appears at a temperature of 400 °C in our experiments. At this temperature, the averaged velocity increases by about 28 percent compared with a room-temperature sphere.

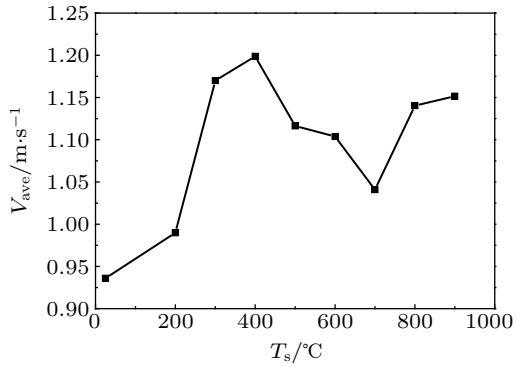


Fig. 2. Average velocities of different-temperature sphere falling into 25-°C water.

The surface state of a sphere has a great influence on the drag characteristics of the sphere moving into water. The surface flow states are different for different sphere temperatures as shown in Fig. 3. In Fig. 3(a), the sphere surface is surrounded by a large number of small bubbles produced by vaporization, in which case the initial sphere temperature is 400 °C. When the initial sphere temperature is 600 °C, large bubbles or vapor shells are formed, and they grow and collapse intensively as shown in Fig. 3(b).

When the initial temperature of the sphere reaches 800 °C, vapor bubbles get together to form a vapor layer, which separates the sphere from the surrounding water. The thermal conductivity of vapor is much lower than that of water, so the boiling phenomenon becomes gentle as shown in Fig. 3(c). The vapor layer is unstable, thin and coarse in Fig. 3(c) and differs from the stable, thick and smooth vapor layer formed in high temperature water. In the low temperature water, the stable film boiling is not easy to happen as described by Yagov *et al.*[21] In our experiments, for spheres falling into the 25-°C water, the boiling states are in the nucleate boiling regime (as shown in Figs. 3(a) and 3(b)) and the unstable film boiling regime (as shown in Fig. 3(c)).

We suspect that the lubrication and the disturbance of the vapor are the two main reasons for reducing the drag. The lubrication can reduce the frictional drag. It can also reduce the pressure drag in some cases, such as the lubrication of the vapor layer as described by Vakarelski *et al.*[17] The disturbance of the vapor can increase the turbulence of the flow which can make the separation point move towards the rear of the sphere and reduce the drag. Different boiling states have different drag reduction effects. The gentle nucleate boiling can reduce more drag than the violent nucleate boiling as shown in Figs. 2 and 3. The velocity and temperature of the sphere will be changed during falling into water, so it is not easy to quantitatively study the effect of drag reduction.

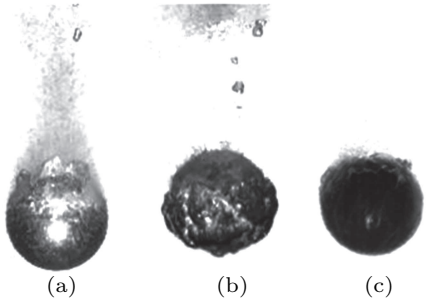


Fig. 3. Surface states of the spheres at 20-cm underneath water surface at $T_s = 400$ °C (a), 600 °C (b), and 800 °C (c), with water temperature maintained at 25 °C in all cases.

Figure 4 shows the falling velocity V varying with falling time t for a room-temperature sphere falling into room-temperature water. The sphere falling into water is affected mainly by gravity and water resistance. At the beginning of the falling process, the velocity is low, and thus leading to low drag of the water. The velocity increases when the sphere moves downward until fluid drag is equal to gravity. Then the sphere will fall approximately at a constant velocity. The exponential function: $V(t) = V_T\ (1 - e^{-t/\tau})$ used by Lyotard *et al.*[22] fits well with the velocities obtained by the video clips. The τ and V_T are constants, and V_T can be used to predict the terminal velocity during the fall. In this trial, the sphere reaches the terminal velocity $V_T = 1.06$ m/s at about $t = 0.4$ s and τ is 0.079 in this case.

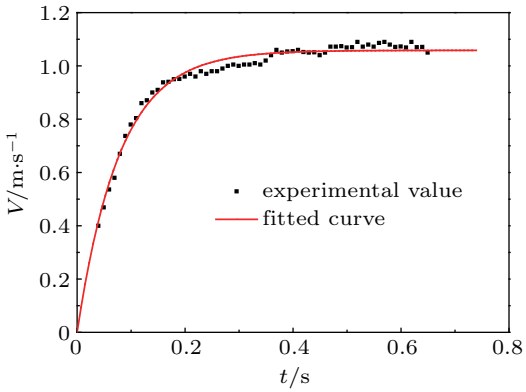


Fig. 4. (color online) Falling velocity of the sphere varying with falling time at $T_w = 25$ °C and $T_s = 25$ °C, with black points representing experimental values obtained by the video clips and red line denoting fitted curve from formula $V(t) = V_T\ (1\,e^{-t/\tau})$.

The drag coefficient of the sphere is $C_D = 2F_D/(\pi R^2 \rho V^2)$. Here F_D is the drag force and ρ is the fluid density. When the sphere reaches its terminal velocity, the drag coefficient can be defined as

$$C_D = [8(\rho_s \rho)gR]/(3\rho V_T^2), \tag{1}$$

where g is gravitational acceleration. The width of the tank is 15 times the diameter of the sphere. Therefore, we neglect the influence of the water tank sidewall effect on the velocity of the sphere. For $T_w = 25$ °C, $T_s = 25$ °C, the drag coefficient calculated by using Eq. (1) is $C_D = 0.51$ when the sphere reaches its terminal velocity.

Figure 5 shows that the change of the falling velocity V with falling time t of a sphere in nucleate boiling regime at $T_w = 25$ °C, $T_s = 400$ °C. The velocity of the sphere increases and reaches its maximum value at about $t = 0.4$ s. Then the velocity decreases until the sphere reaches the bottom of the water tank. The velocity variation of the sphere in the nucleate boiling regime and the room-temperature sphere are different. The exponential function used in Fig. 4 cannot be used to estimate the falling velocity of the sphere in the nucleate boiling regime. In Fig. 5 we find that the cubic polynomial function can fit the experimental values well.

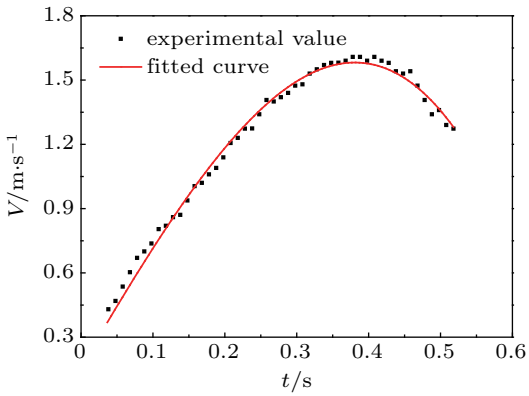


Fig. 5. (color online) Falling velocity of sphere varying with falling time at $T_w = 25$ °C and $T_s = 400$ °C. Black points represent experimental values obtained by video clips and the red line refers to fitted curve by using cubic polynomial formula: $V(t) = 0.32 + 3.62t + 7.15t^2 - 20.56t^3$.

The maximum falling velocity shown in Fig. 5 is about $V_{max} = 1.6$ m/s, and it is about 51 percent larger than that of the room-temperature sphere shown in Fig. 4. At $V = V_{max} = 1.6$ m/s, the falling velocity reaches its extreme value, and the acceleration is approximately equal to 0. We calculate the drag coefficient at this time by using Eq. (1). The drag coefficient calculated is $C_D = 0.23$, which is much lower than the drag coefficient of the room-temperature sphere shown in Fig. 4. The nucleate boiling has a significant effect on drag reduction.

The falling velocity cannot keep its maximum value, and the drag reduction effect of the nucleate boiling weakens after $t = 0.4$ s, leading to the increase of fluid drag. The velocity and temperature of the sphere change with falling time, so do the nucleate boiling states. It is difficult for us to study the drag reduction characteristics of the sphere in nucleated boiling regime at different drop times. We can conclude that in this nucleate boiling case shown in Fig. 5, the drag coefficient can be as low as 0.23.

3.2. Influence of water temperature

Figure 6 shows the plots of average velocity of the sphere falling into water versus the sphere temperature for the water temperature 25 °C, 50 °C, 80 °C, and 95 °C. For $T_w = 25$ °C, the average velocity of the sphere slightly increases with water temperature increasing. At $T_s = 25$ °C, the water cannot vaporize. The dynamic viscosity of the water μ decreases with water temperature increasing. The Reynolds number $Re = \rho V_0 R_0/\mu$ increases with the water temperature increasing. The drag coefficient C_D decreases with the increase of Re until Re reaches the subcritical range $5 \times 10^3 \leq Re \leq 3 \times 10^5$. In the initial stage of the fall, the falling velocity is small which leads to a low Re. So for high temperature water, the drag coefficient of the sphere is smaller in the initial falling stage, leading to a slightly lager averaged velocity in the whole falling stage.

The data points inside the dashed ellipse represent the stable film boiling cases. When both of the water temperature and the sphere temperature are high, a stable and smooth vapor layer can be easily formed by converging the vaporized bubbles. The average velocities of the sphere with temperature $T_s = 800$ °C in an unstable film boiling regime for water temperature $T_w = 25$ °C and 50 °C, are close to each other. For $T_s = 300$ °C and 500 °C, the average falling velocity decreases with water temperature increasing. In the nucleate boiling state, the violent boiling and large bubbles have less drag reduction effect than the gentle boiling and small bubbles. The average falling velocity of the sphere in the stable film boiling regime is larger than that of the room-temperature sphere and smaller than that of the sphere in nucleate boiling and unstable film boiling regime as shown in Fig. 6. In the stable film boiling regime, the average velocity of the sphere in 95-°C water is smaller than that in 80-°C water, and the temperature of the sphere has only a little effect on the average velocity.

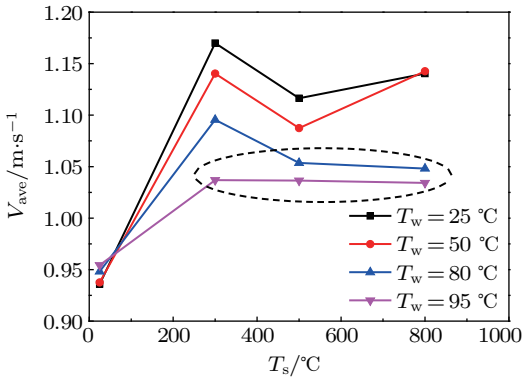


Fig. 6. (color online) Plots of average velocity versus falling sphere temperature into different-temperature water.

In Fig. 7 we present the change of the falling velocity V dependent on falling time t for a sphere in stable film boiling regime at $T_w = 95$ °C, $T_s = 500$ °C. The exponential function: $V(t) = V_T\ (1\,e^{-t/\tau})$ fits well to the experimental velocity values, which is similar to the case shown in Fig. 4. The terminal velocity predicted by the exponential function is $V_T = 1.32$ m/s. The τ is 0.156 in this case. The experimental velocity value at the bottom of the tank is just close to 1.32 m/s, and there is still a small trend of acceleration. The maximum velocity of the sphere in stable film boiling regime shown in Fig. 7 is about 24 percent larger than that of the room-temperature sphere shown in Fig. 4, but it is smaller than

the 51 percent of the value for the nucleate boiling case shown in Fig. 5. We ignore the small acceleration of the sphere at the bottom of the tank. The drag coefficient is $C_D = 0.33$ calculated by using Eq. (1). The drag coefficient of the sphere in stable film boiling regime at its maximum velocity shown in Fig 7 is smaller than 0.51 for the room-temperature sphere shown in Fig. 4 and lager than 0.23 for the sphere in nucleate boiling regime shown in Fig. 5. The maximum velocity V_{max} and the corresponding drag coefficient C_D for the room-temperature sphere, the nucleate boiling and the stable film boiling cases are summarized in Table 2.

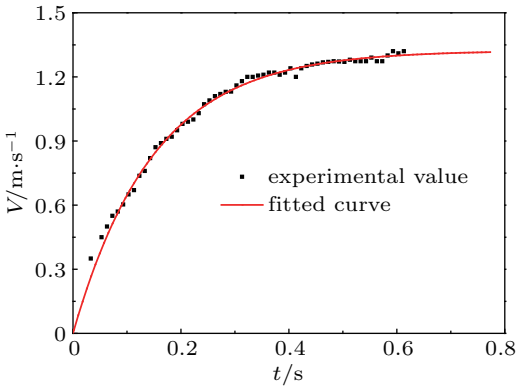


Fig. 7. (color online) Plots of falling velocity of the sphere versus falling time at $T_w = 95$ °C and $T_s = 500$ °C. Black points denote experimental values obtained by video clips and the red line refers to fitted curve by using formula: $V(t) = V_T\,(1\,e^{-t/\tau})$.

Table 2. Maximum velocities and their corresponding drag coefficients for different values of T_w and T_s.

T_w/°C	T_s/°C	V_{max}/(m/s)	C_D
25	25	1.06	0.51
25	400	1.6	0.23
95	500	1.32	0.33

Vakarelski *et al.*[17–19] presented that the terminal velocities of the spheres in stable film boiling regime are much higher than those of the spheres in nucleate boiling regime. They also presented that the nucleate boiling just has a little effect on the terminal velocity. The test liquids were water with different temperatures and perfluorinated fluids with different viscosity. In their experiments, the height of the tank was in a range from 1.6 m to 2 m. The temperature of the sphere dropped quickly when falling in the liquid, and the intensity of the nucleate boiling was weak when the sphere reached the bottom of the tank. So it is hard to evaluate the drag reduction effect of the nucleate boiling in their experiments.

The height of the water tank in our experiment is 0.6 m. The nucleate boiling is more intensive when the sphere reaches the bottom of the tank than that in the experiments by Vakarelski *et al.*[17–19] As shown in Fig. 6, the average velocity of the sphere in nucleate boiling regime is larger than that of the sphere in stable film boiling regime. The nucleate boiling has a larger drag reduction effect in the present study.

Figure 8 shows the flow states around the sphere at 40 cm underneath the water surface for a room-temperature sphere (Fig. 8(a)), a sphere in stable film boiling regime (Fig. 8(b)) and a sphere in nucleate boiling regime (Fig. 8(c)). The flows in Fig. 8 are in the subcritical Reynolds number range. In this regime, the total drag is dominated by the pressure drag and the frictional drag accounts for only a small proportion. The pressure drag is caused by flow separation. For a room-temperature sphere, the flow separates at about the equator of the sphere and the drag coefficient is approximately constant.

In Fig. 8(a), rhodamine B is used to visualize the flow field. The maximum diameter of the bluish red wake is slightly larger than the diameter of the sphere. The flow separation position is just a little far underneath the equator of the sphere, which is consistent with the Achenbach's experimental results.[23]

In Fig. 8(b), a stable and smooth vapor layer is generated around the sphere. The sphere looks smaller than its actual size due to the light refraction. The intensity of the heat transfer in this regime is weak, we cannot see the discrete vapor bubbles in the wake of the sphere. Vakarelski *et al.*[17] used a perfluorinated fluid with a low boiling point and a low vaporization heat capacity, the bubbles in the wake acted as tracer particles and helped to identify the flow separation point. They presented that the vapor layer can make the flow separation point move to the rear of the sphere and reduce the drag. The drag reduction effects of the stable film boiling in the Vakarelski *et al.*'s study[17–19] are more significant than that in the present study. Vakarelski *et al.*[17–19] demonstrated that the drag reduction effect in the stable film boiling state is related to the Reynolds number of the flow. The water tank in our experiments is short and the velocity cannot increase sufficiently, thus leading to low *Re*.

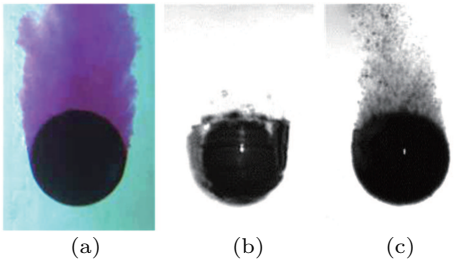


Fig. 8. (color online) Flow states around spheres at 40 cm underneath water surface at (a) $T_w = 25$ °C and $T_s = 25$ °C; (b) $T_w = 95$ °C and $T_s = 500$ °C; (c) $T_w = 25$ °C and $T_s = 400$ °C.

In Fig. 8(c), a large number of micro vapor bubbles are formed due to the high heat transfer intensity in the nucleate boiling regime. With the help of visible bubbles, we can see that the flow separates in the rear of the sphere, thus leading

to low pressure drag. The drag reduction effect of the nucleate boiling is greater than that of the stable film boiling as shown in Fig. 6.

As shown in Fig. 8(b), the vapor layer becomes thicker in the rear of the equator of the sphere. We suspect that when the falling velocity is not high enough, the vapor layer may accumulate in the rear of the equator of the sphere and make the flow separate. While for the nucleate boiling case, the discrete vapor bubbles are not easy to accumulate, the flow separation point becomes closer to the tail of the sphere than the scenario in the stable film boiling case, which leads to a high drag reduction effect.

3.3. Stability of fall trajectory

In Fig. 9 we show the falling trajectories of room-temperature spheres, spheres in the nucleate boiling regime and spheres in the stable film boiling regime. We present three independent experimental results for each case. The division of horizontal axis is twice that of the vertical axis in order to see the deviation of the trajectory clearly.

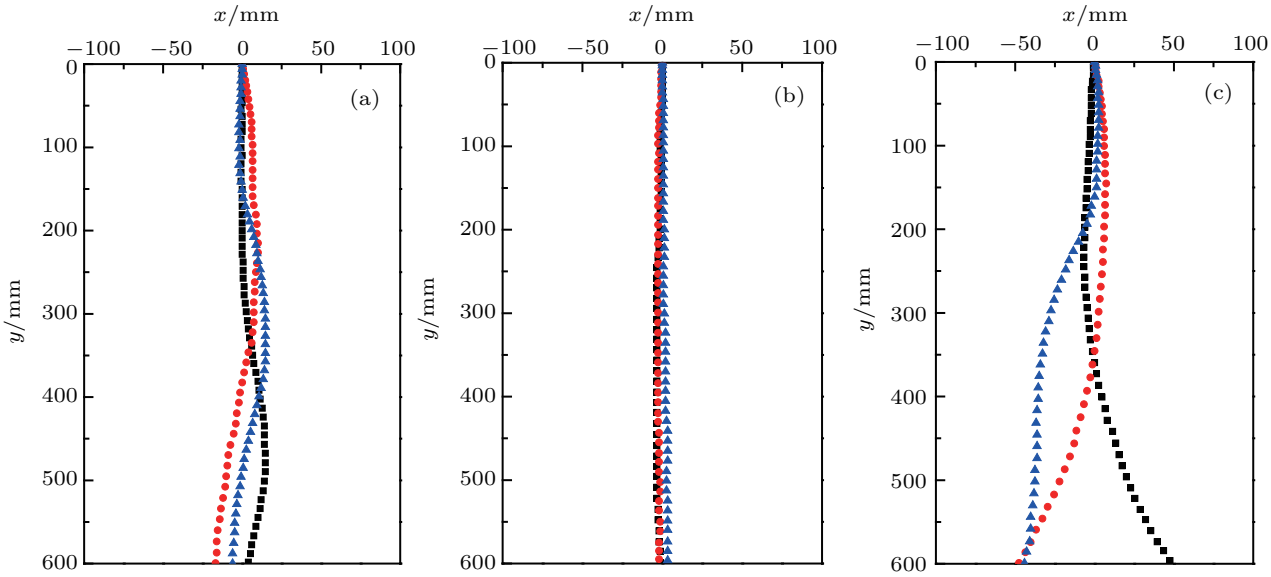


Fig. 9. (color online) Comparison among trajectories of different-temperature spheres falling into different-temperature water: (a) $T_w = 25$ °C and $T_s = 25$ °C; (b) $T_w = 95$ °C and $T_s = 500$ °C; (c) $T_w = 25$ °C and $T_s = 400$ °C. In each panel, different symbols represent different independent trials for the same water and sphere temperature.

In accordance with Vakarelski *et al.*'s study[18] the trajectories of the falling spheres in stable film boiling regime (Fig. 9(b)) are more straight than those of the room-temperature spheres (Fig. 9(a)). For a room-temperature sphere, the flow separation occurs near the sphere's equator, asymmetric periodic vortex shedding appears behind the separation point, thus leading to a large lateral force. The lateral force causes the sphere to laterally deflect. According to the discussion in Subsection 3.2, for a sphere in stable film boiling regime, the flow separation occurs in the rear of the sphere. Comparing with a room-temperature sphere, the vortex area of a sphere in stable film boiling regime is narrow which leads to a smaller lateral force. So the falling movement is more stable for a sphere in stable film boiling regime.

In the present study, we also discuss the moving stability of the spheres in nucleate boiling regime. Like the behavior of a sphere in film boiling regime, for a sphere in nucleate boiling regime, the flow separation occurs in the rear of the sphere and the vortex area is narrower than that of a room-temperature sphere. The wake appears streamlined as shown in Fig. 8(c). But we find that the lateral displacements of the spheres in nucleate boiling regime (Fig. 9(c)) are larger than those of the room-temperature spheres (Fig. 9(a)). We suspect that the large deviation is caused by the disturbance of vapor bubbles or the growth and collapse of the vapor shells.

4. Conclusions

We investigate the boiling effect on drag reduction during the falling process of a sphere in water. In 25 °C water, with the increase of the temperature of the sphere, the average falling velocity first increases and then decreases until the sphere temperature reaches 700 °C; the average velocity increases while the sphere temperature continues rising. In our experiments, the maximum average velocity appears at $T_s = 400$ °C and $T_w = 25$ °C and increases by about 28 percent compared with that for a room-temperature sphere. The drag reduction effect of the stable film boiling is lower than that of the nucleate boiling. In the nucleate boiling regime, the average velocity decreases with water temperature increasing, the drag of the sphere with gentle boiling intensity is smaller.

The exponential function: $V(t) = V_T\ (1\,e^{-t/\tau})$ fits well to the experimental velocities for room-temperature spheres and spheres in stable film boiling regime. The velocity of

the sphere in nucleate boiling regime at $T_s = 400$ °C and $T_w = 25$ °C increases to a maximum value at about $t = 0.4$ s. Then the velocity decreases until the sphere reaches the bottom of the water tank. The maximum velocity of the sphere in nucleate boiling regime is about 51 percent larger than that of the room-temperature sphere.

The flow separation position is a little lower than the equator of the room-temperature sphere. For heated spheres, the separation positions will move to the rear of the sphere. Comparing with the sphere in stable film boiling regime, for the sphere in nucleate boiling regime the discrete vapor bubbles are not easy to accumulate, thus leading to lower pressure drag. Compared with the room-temperature spheres, the spheres in stable film boiling regime have good moving stability and the spheres in nucleate boiling regime have large lateral displacements.

References

[1] Yang S Q and Dou G 2010 *J. Fluid Mech.* **642** 279
[2] Li F C, Wang L and Cai W H 2015 *Chin. Phys. B* **24** 074701
[3] Guan X L, Wang W and Jiang N 2015 *Acta Phys. Sin.* **64** 094703 (in Chinese)
[4] Elbing B R, Winkel E S, Lay K A, Ceccio S L, Dowling D R and Perlin M 2008 *J. Fluid Mech.* **612** 201
[5] Qin S J, Chu N, Yao Y, Liu J T, Huang B and Wu D Z 2017 *Phys. Fluids* **29** 037103
[6] Ceccio S L 2010 *Ann. Rev. Fluid Mech.* **42** 183
[7] Wang B, Wang J D, Chen D R, Sun N and Wang T 2017 *Chin. Phys. B* **26** 054701
[8] Rothstein J P 2010 *Ann. Rev. Fluid Mech.* **42** 89
[9] Mchale G, Newton M I and Shirtcliffe N J 2010 *Soft Mater.* **6** 714
[10] Jetly A, Vakarelski I U, Thoroddsen and S T 2018 *Soft Matter* **14** 1608
[11] Bradfield W S, Barkdoll R O, Byrne J T 1962 *Int. Heat Mass Transfer* **5** 615
[12] Quéré D 2013 *Ann. Rev. Fluid Mech.* **45** 197
[13] Saranadhi D, Chen D Y, Kleingartner J A, Srinivasan S, Cohen R E and Mckinley C H 2016 *Sci. Adv.* **2** e1600686
[14] Hof B 2017 *Nature* **541** 161
[15] Zvirin Y, Hewitt G R and Kenning D B R 1990 *Exp. Heat Transfer* **3** 185
[16] Gylys J, Skvorcinskiene R, Paukstaitis L, Gylys M and Adomavicius A A 2015 *Int. Heat Mass Transfer* **89** 913
[17] Vakarelski I U, Marston J O, Chan D Y C and Thoroddsen S T 2011 *Phys. Rev. Lett.* **106** 214501
[18] Vakarelski I U, Chan D Y C and Thoroddsen S T 2014 *Soft Matter* **10** 5662
[19] Vakarelski I U, Berry J D and Chan D Y C 2016 *Phys. Rev. Lett.* **117** 114503
[20] Berry J D, Vakarelski I U, Chan D Y C and Thoroddsen S T 2017 *Phys. Fluids* **29** 107104
[21] Yagov V V, Lexin M A, Zabirov A R and Kaban'kov O N 2016 *Int. Heat Mass Transfer* **100** 98
[22] Lyotard N, Shew W L, Bocquet L and Pinton J F 2007 *Eur. Phys. J. B* **60** 469
[23] Achenbach E 1972 *J. Fluid Mech.* **54** 565